OPTICAL EMISSION IN THE BEAM OF STELLAR JETS: A POSSIBLE MECHANISM

F. BACCIOTTI,[1] C. CHIUDERI,[1] AND A. POUQUET[2]

ABSTRACT

We propose a mechanism for the optical emission observed in the beam section of stellar jets based on the stability properties of circularly polarized Alfvén waves propagating in the partially ionized medium filling the jet's channel. We first derive the relevant magnetohydrodynamic equations, which include the Hall term for such a partially ionized medium, a term which give rise to dispersive effects. Quasi-equipartition of thermal and magnetic energies is assumed, and the model is developed in the one-dimensional approximation but keeping the three components of the vectorial fields. Mild compressions or very weak shocks occur in the flow when instabilities develop, depending on the relative sign of the angular momentum of the underlying accretion disk and the external magnetic field. Simulations performed under quite general conditions show that the temperature/density perturbations associated with the instability are consistent with the average luminosity contrast observed in the jet's beam between bright knots and interknot regions.

Subject headings: ISM: jets and outflows — MHD — polarization — shock waves — stars: pre–main-sequence

1. INTRODUCTION

Stellar Herbig-Haro (HH) jets have been the subject of intense investigation over past years (see, for example, the reviews by Mundt 1993; Reipurth & Heathcote 1993; Raga 1991a, Königl 1995). These nebulosities associated with young stellar objects (YSOs) trace highly collimated gas that accelerates away from the star at several hundred kilometers per second. They are generally detected at optical wavelengths, and their common appearance is that of a narrow chain of bright knots ("jet") followed by one or more bow-shaped terminal features aligned with the jet section. All structures produce emission-line spectra which are believed to form in the cooling regions behind shock fronts, the terminal bow shock being characterized by higher excitation ($v_{shock} \sim 150$ km s^{-1}), while the jet section shows an extremely low excitation type of emission (witnessed by the high value of the [S II]/Hα ratio), with typical shock velocities of 10–30 km s^{-1}.

The purely hydrodynamical models so far proposed in order to give justification to the peculiar morphology and emission properties of the nodular linear section (on which we concentrate our attention) are of three distinct types. One type involves static periodic patterns of oblique internal shocks, which invariably form when a supersonic jet exits from a De Laval nozzle; a second based on the assumption that the matter is ejected with periodic velocity fluctuations from the circumstellar environment, thus forming a chain of traveling working surfaces in the beam; the last one, finally, invokes the action of Kelvin-Helmholtz instabilities at the border of the flow channel as responsible for the formation of weak traveling shocks internal to the beam. Although a lot of work has been devoted to the topic, none of the proposed approaches, is capable of reproducing the observed properties in a satisfactory way (see Bacciotti,

Chiuderi, & Oliva 1995, hereafter BCO, for an extended discussion). The main difficulty with such models is the identification of the mechanism capable of generating long-lived shock fronts traveling at high velocity, which produce simultaneously very low excitation spectral features. A possible resolution could come from the introduction in the models of magnetic fields, that could play an important role in lowering the gas excitation efficiency of shock fronts that may eventually form inside the beam. Magnetic fields are surely present in the jet which propagates in a magnetized molecular environment, and several models have recently been proposed that invoke magnetic fields as a crucial ingredient of the outflow acceleration and collimation processes (see, for example, Uchida & Shibata 1985; Pudritz & Norman 1986; Lovelace, Wang, & Sulkanen 1987; Lovelace, Berk, & Contopoulos 1991; Pelletier & Pudritz 1992). The outflows are, as a rule, roughly parallel to the nebular large-scale field (Strom et al. 1986; Ray 1987; Reipurth 1989). Direct measurement of the intensity of the magnetic field inside the jet itself is impeded by the large internal velocity dispersion of the optical lines: typical values for the dispersion found in lines from YSO jets range between 15 and ~ 100 km s^{-1}, large enough to render the measurement of Zeeman splitting practically impossible at optical and IR wavelengths, unless the magnetic fields exceed several hundred gauss. To arrive at an estimate of the intensity B of the magnetic field in the jet, we shall make the assumption that the magnetic energy density is in quasi-equipartition with the thermal forms of energy. Assuming that most of the matter in the jet has a mean temperature of 2000 K and a mean numerical density $n_H \sim 10^4$ cm^{-3} (Hartigan, Morse, & Raymond 1994; BCO), a value of $B \sim 200$ μG is obtained, which leads to an Alfvén speed of ~ 5 km s^{-1}. In most of the magnetic acceleration models previously mentioned, the magnetic surfaces have an hourglass shape, with the flattened mass accretion envelope situated on the central perpendicular plane of the hourglass. Due to the high thermal pressure in the disk, the field lines are more or less tightly connected to it, and it is therefore likely that while the accretion disk rotates around the pro-

[1] Dipartimento di Astronomia e Scienza dello Spazio, Università di Firenze, Largo Enrico Fermi 5, I-50125 Firenze, Italy.
[2] Observatoire de la Côte d'Azur, CNRS URA 1362, BP 4229, 06304 Nice Cedex 4, France.

tostar, circularly polarized Alfvén waves are excited that can propagate to large distances. The aim of this paper is to analyze the properties of the fluid motion of the jet gas in the presence of MHD waves and the stability of such waves with respect to amplitude perturbations in a regime appropriate for the physical conditions of a YSO jet, and at large spatial and temporal scales.

The optical lines coming from HH objects indicate that the jet gas is mainly in atomic form. Recent studies, in addition, have demonstrated that the degree of ionization in the linear jet section varies from moderate to low: Raga (1991b), was the first to realize that the hydrogen ionization fraction in jets is most likely around 10%; this suggestion has been confirmed by the new model-independent spectral diagnostic technique described in BCO, that gives for the linear section of the HH 34 and HH 111 jets values around 7%–10% (BCO; Bacciotti, Eislöffel, & Ray 1996a), while for the optical outflow from the T Tauri star RW Aurigae, a degree of ionization around 10%–20% has been found (Bacciotti, Hirth, & Natta 1996b). We thus adopt for the description of the propagation of waves in the collimated section of the jet a model based on the MHD equations using a generalized Ohm's law appropriate for the case of a weakly ionized medium. Since the relevant equations contain nonlinear terms coupling Alfvén and sonic waves, the instabilities that may form as a consequence of an initial perturbation of the magnetic wave amplitude (due, for example, to a sudden release of accumulated magnetic twist), may produce steepened hydrodynamic features that can degenerate into traveling shock fronts. In addition, it will be proved that partial ionization stresses the dynamical importance of the Hall effect: it is its dispersive character that competes with the steepening of velocity profiles by the hydrodynamical nonlinearities. In conclusion, as we shall show, the stability properties of circularly polarized Alfvén waves most likely excited by the rotation of the accretion disk will allow for the presence of traveling weak shocks in the flow. We derive the equations in § 2 taking into account the simplifications that can be drawn using several observational facts. We analyze these equations both analytically and numerically in § 3 in the context of a regime stressing the large-scale dynamics and the quasi-equipartition between magnetic and thermal energy densities, following a previous analysis by Hada (1993) in the context of solar wind physics. The paper concludes with a discussion in § 4.

2. THE HALL MHD EQUATIONS FOR A PARTIALLY IONIZED MEDIUM

The medium that constitutes the jet is a weakly ionized plasma, the neutrals making up about 90% of the total number density. Even so, the ionization of the jet is much larger than that of the embedding cloud, typically of the order of 10^{-4} to 10^{-6}. This fact has important consequences when we are choosing the regime appropriate for describing the jet's properties, as we shall point out later on.

We start by considering a system composed of three fluids, corresponding to electrons (e), ions (i), and neutrals (n). We further restrict the analysis to a pure hydrogen plasma, so that $m_i \simeq m_n$. The plasma must be electrically neutral on average, which implies $n_i \simeq n_e$ everywhere. The derivation of the appropriate three-fluid equations and their reduction to one-fluid form is standard; it can be found, e.g., in Braginskii (1965), to which we refer the reader for details. In the following we shall simply recall the steps relevant to

our discussion. The level of ionization of the plasma is measured by the ratio

$$\xi = \frac{n_i}{n_i + n_n} , \qquad (1)$$

which can a priori be space-dependent (in fact, it decreases along the jet axis, as shown in Bacciotti et al. 1996b, 1996a). The one-fluid plasma matter density ρ and average speed U are defined as

$$\rho = \sum_s \rho_s \quad (s = e, i, n) ,$$

and

$$\rho U = (\sum_s \rho_s u_s) ,$$

where the ρ_s are the single-species densities and the u_s are the corresponding average velocities.

By adding the continuity and momentum equations for the three fluids, we easily obtain their one-fluid form:

$$\frac{\partial \rho}{\partial t} + \nabla \cdot (\rho U) = 0 ,$$

$$\rho \left[\frac{\partial U}{\partial t} + (U \cdot \nabla) U \right] = -\nabla P + qE + \frac{1}{c} (j \times B) ,$$

where $q = e(n_i - n_e)$ is the charge and $j = en_i(u_i - u_e)$ is the current density. It is easily shown that the electric field term qE is always negligible in the MHD regime.

To define the pressure term, we first express the single-species velocities as $u_s = U + w_s$ and then define $[\rho \langle w_k w_l \rangle]_s = P_s \delta_{kl}$, where the angular brackets denote the average over the random velocities distribution function. Finally, $P = \sum_s P_s$.

The dissipative and dispersive effects come into play through the so-called generalized Ohm's law. Neglecting terms of the order m_e/m_i and proceeding in the standard way, we arrive at (see Braginskii 1965, eq. [7.12])

$$E + \frac{1}{c} (u_i \times B) - \frac{1}{en_i} \nabla P_e = \frac{j}{\sigma} + \frac{1}{en_i c} (j \times B) , \qquad (2)$$

where σ is the electrical conductivity.

In order to use equation (2) in conjunction with the equation of motion, it is necessary to express the quantities u_i, P_e, and n_i in terms of the global quantities U, P, and ρ. From the definitions, and assuming equal temperatures for all species we have:

$$u_i = U + (1 - \xi) u_D ,$$

where $u_D = u_i - u_n$ is the "drift" velocity between neutrals and ions, and

$$\rho = \frac{m_i n_i}{\xi} , \quad P = P_e \left(1 + \frac{1}{\xi} \right) .$$

Adapting to our notation the expression for u_D given by Braginskii (1965) (his eq. [7.10]), we have

$$u_D \simeq \frac{2(1 - \xi)}{n_i n_n m_i \alpha'_{in}} \left[-\nabla P_e + \frac{1}{c} j \times B \right] . \qquad (3)$$

The "momentum transfer rate coefficient" α'_{in} can be found in Draine, Roberge, & Dalgarno (1983), who give, for small values of $u_D = |u_D|$,

$$\alpha'_{in} \simeq 2 \times 10^{-9} \text{ cm}^3 \text{ s}^{-1} .$$

After an estimate of the order of magnitude of the terms appearing in equation (3), we arrive at the following expression for u_D:

$$u_D \simeq \frac{(1 - \xi)^2 10^9}{\xi n_n^2 m_i} \frac{1}{4\pi} \frac{B^2}{L} \text{ cm s}^{-1} ,$$

where L is the scale length for variations of B. Using the values mentioned in § 1, we finally get $u_D \simeq 10^{17}/L$ cm s^{-1}.

We therefore see that for every reasonable value of L, $u_D \ll u_i$. This estimate is further strengthened by the observations of spectral lines from both ionized and neutral species that indicate $u_n \simeq u_i$. The above arguments then allow us to simply replace u_i by U in the generalized Ohm's law that now reads:

$$E + \frac{1}{c} (U \times B) - \frac{m_i}{(1 + \xi)e\rho} \nabla P = \frac{j}{\sigma} + \frac{m_i}{e\rho\xi} \frac{1}{c} (j \times B) . \quad (4)$$

From an order-of-magnitude estimate of the various terms we conclude that both the Joule dissipative term j/σ and the pressure gradient term can be safely neglected in the conditions under study. The last term on the right, the so-called Hall term, must instead be retained when the drift velocity of the electrons with respect to the ions is of the same order as the ion's speed. This occurs in a partially ionized medium due to the different slowing down of the two charged species caused by the collisions with the neutrals.

We can thus retain in Ohm's law the usual induction term and the Hall term; this leads to the following induction equation:

$$\frac{\partial B}{\partial t} = \nabla \times (U \times B) - \frac{m_i}{e} \nabla \times \left(\frac{1}{\rho\xi} j \times B \right) . \quad (5)$$

The latter equation, together with the continuity and momentum equations previously written, constitutes the starting point of our analysis corresponding to the three-fluid approach with approximately equal ion and neutral velocities. Note the factor $1/\xi$ in the Hall term. From a physical point of view it can be said that at fixed ion density, when neutrals are present, the ions and the electrons are slowed down differently in a collision with a neutral, obviously because of their different mass, and thus the current, proportional to the difference of velocities between ions and electrons, is larger, hence there is a stronger Hall effect which translates in the equations by the $1/\xi$ factor. Indeed, one recovers the usual MHD equations for a fully ionized fluid for $\xi \to 1$ (no neutrals present). However, we stress that the above equation is not valid in the opposite limit of a very weakly ionized plasma such as for the interstellar medium, where ξ can be as low as $\sim 10^{-6}$. In that case u_D becomes much larger and the replacement of u_i by U is no longer applicable. A new dominant term then appears corresponding to the ambipolar drift. The apparent paradox (that in the limit $\xi \to 0$ the Hall term is negligible) comes from the fact that, hidden in this formulation of the equation, the current, of course, is proportional to the ion density, which in this limit would become negligible.

3. ANALYSIS OF THE MODEL

3.1. Basic Equations

We consider a protostar surrounded by a rotating accretion disk embedded in a uniform magnetic field, with a double jet emanating in two opposite directions. The rotation of the disk excites polarized Alfvén waves that propagate within the beam of the jet—a weakly ionized medium ($\xi \sim 0.1$). We propose to study the stability properties of such waves in the framework of the equations developed in the preceding section. As a first approximation, we consider a slab geometry (three components of the vectors, with only one-dimensional dependence of variables), and a constant ionization fraction ξ.

In the following we will use a nondimensional form of the modified MHD equations derived in the previous section. They read:

$$\frac{\partial \rho}{\partial t} + \nabla \cdot (\rho U) = 0 ,$$

$$\rho \left[\frac{\partial U}{\partial t} + (U \cdot \nabla)U \right] = -\nabla \left(P + \frac{|B|^2}{2} \right) + (B \cdot \nabla)B ,$$

$$\frac{\partial B}{\partial t} = \nabla \times (U \times B) - \frac{1}{\xi} \nabla$$

$$\times \left[\frac{1}{\rho} (\nabla \times B) \times B \right],$$

$$\nabla \cdot B = 0 . \quad (6)$$

Here ρ is the total density (ions + neutrals) normalized to ρ_0, P is the total pressure normalized to $B_0^2/4\pi$, $B = (h, b_y, b_z)$ is the magnetic field normalized to B_0, and $U = (u, v_y, v_z)$ is the velocity of the center of mass normalized to the Alfvén speed $c_A = (B_0^2/4\pi\rho_0)^{1/2}$, where ρ_0 and B_0 are the mean density and mean magnetic field in the jet; B_0 is assumed to be parallel to the x-axis. Time and space are thus normalized to Ω_i^{-1} and c_A/Ω_i, where $\Omega_i = eB_0/m_i c$ is the ion gyrofrequency.

To close the above set, an energy equation must be specified. Since this paper is intended as a first approach to the study of the competition between nonlinear and dispersive effects in weakly ionized plasma, even a simple adiabatic law $d(P\rho^{-\gamma})/dt = 0$ could suffice. However, we have also tried to mimic the effect of heating and radiation by replacing the specific-heat ratio γ by a variable parameter λ. The justification for such a procedure relies upon the fact that in most astrophysical gaseous nebulae heating and cooling timescales are much shorter than dynamical timescales, therefore the energy equation practically reduces to an equilibrium between the heating and cooling processes active in the gas: Elmegreen (1991) has shown that, by linearizing the full energy equation around an equilibrium state, it is actually possible to compute λ when the heating and radiation terms are expressed as power laws of the basic thermodynamic quantities. For example, Vazquez, Passot, & Pouquet (1995), in their simulations of ISM properties in star formation regions, assume as their main source of heating the ubiquitous, yet of uncertain origin, diffuse UV radiation field, which is believed to provide the source of ionization for the warm ionized medium in the ISM: they set the corresponding heating rate proportional to ρ, while for the radiation losses they use a piecewise cooling curve proportional to different powers of the temperature, depending on the temperature range. Adopting tentatively the same approach as in Vazquez et al. (1995) (see also Passot, Vazquez, & Pouquet 1996), we find $\lambda = \frac{1}{3}$, since, for the temperature range we are interested in, the radiative

cooling rate turns out to be proportional to $\rho^2 T^{1.5}$ (Dalgarno & McCray 1972). An empirical justification of such a choice can in fact also be found in the results of the above-mentioned ISM simulations (Vazquez et al. 1995; Passot, Vazquez, & Pouquet 1995) that use the full energy equation and yet result in a scatter plot for which $P \sim \rho^{0.3}$ is a good fit, both in the unmagnetized and in the magnetized cases. We shall therefore adopt as our energy equation

$$\frac{d}{dt}(P\rho^{-\lambda}) = 0 \tag{7}$$

and check the sensitivity of the results to λ both analytically and numerically.

As already mentioned in § 1, we assume that all physical variables depend only on the coordinate x, but we maintain the full three-dimensional character of vector fields. The star is located at the origin, and it is surrounded by an accretion disk that lies on the y-z plane; the bipolar jet flows along the $+x$ and $-x$ directions, parallel to the large-scale uniform magnetic field, which has the same (positive) orientation on both sides of the star.

We first introduce the complex variables

$$v = v_y + iv_z, \quad b = b_y + ib_z$$

and cast equation (6) into the form

$$\frac{\partial \rho}{\partial t} + \frac{\partial}{\partial x}(\rho u) = 0, \quad \rho \frac{dv}{dt} = \frac{\partial b}{\partial x},$$

$$\rho \frac{du}{dt} = -\frac{\partial}{\partial x}\left(P + \frac{1}{2}|b|^2\right),$$

$$\frac{db}{dt} = \frac{\partial v}{\partial x} - b\frac{\partial u}{\partial x} - \frac{i}{\xi}\frac{\partial}{\partial x}\left(\frac{dv}{dt}\right), \tag{8}$$

with $h \equiv 1$.

A medium described by the above system of model equations admits circularly polarized Alfvén waves as linear normal modes. This is easily seen by linearizing the system around a static ($U_0 = 0$) equilibrium state where the normalized magnetic fields and density are $\boldsymbol{B}_0 = (1, 0, 0)$ and $\rho_0 = 1$. Assuming that the first-order quantities vary as exp $[i(kx - \omega t)]$, the linear dispersion relation in the long-wavelength limit turns out to be

$$\omega = -k^2/2\xi \pm k,$$

where $c_A = 1$ in our nondimensional system of units. The k^2 term contained in the dispersion relation reflects the fact that the circularly polarized ($|b| = $ constant) Alfvén waves are modified by dispersive effects.

We wish now to introduce the effect of a weak nonlinearity (we are looking for weak shocks) and see how this modifies the above results. The standard technique to do this is to expand in terms of a small parameter ϵ not only the variables but also the coordinates. This method, called "reductive perturbation expansion," has been successfully applied to the study of the formation of MHD solitons due to the competition between nonlinear steepening and dispersion. For quasi-parallel propagation, and away from equipartition ($c_s^2/c_A^2 \neq 1$, where c_s is the average sound speed), the system of equations (8) reduces to a single nonlinear equation for b, the density and the velocity being given in terms of b only. The equation for b turns out to be the derivative nonlinear Schrödinger (DNLS) equation,

whose properties have been thoroughly investigated by numerous authors (Kaup & Newell 1978; Mjølhus 1978; Mjølhus & Wyller 1986; Spangler & Sheerin 1982; Spangler 1985).

Near equipartition, the system of three standard MHD wave modes (Alfvén and slow and fast magnetosonic) become degenerate, and the equation for b develops a singularity. A new treatment becomes necessary, and the triply-degenerate problem has been solved by Hada (1993) for the fully ionized solar wind plasma. As we see below, an interesting physical consequence of being near equipartition is that the equations for b and v no longer decouple, so that the full nonlinear dynamics is now retained.

From now on, we shall closely follow Hada's (1993) approach, since the only modifications to his basic system of equations are our introduction of the factor $1/\xi$ in the induction equation to take into account the partial ionization of the medium, and the inclusion of a nonzero velocity in the x-direction. We thus write

$$\rho = 1 + \epsilon\rho_1 + \epsilon^2\rho_2 + \cdots,$$

$$P = 1 + \epsilon p_1 + \epsilon^2 p_2 + \cdots,$$

$$u = u_0 + \epsilon u_1 + \epsilon^2 u_2 + \cdots,$$

$$v = \epsilon v_1 + \epsilon^2 v_2 + \cdots,$$

$$h = 1 + \epsilon h_1 + \epsilon^2 h_2 + \cdots,$$

$$b = \epsilon b_1 + \epsilon^2 b_2 + \cdots. \tag{9}$$

In contrast to Hada's (1993) scheme, a constant parallel speed u_0 has been introduced in the basic state to take into account the fact that the waves propagate in a high-speed flow. It is easy to show, however, that this does not change the basic physical properties of the results: the features emerging in the "natural" frame that moves along with the magnetic perturbation are the same in both cases, the only difference being the fact that in Hada's case this frame moves with speed c_A, while in our case it moves practically with the bulk flow, owing to the fact that Alfvén waves are transported by the fluid motion.

As far as the coordinates are concerned, the scaling is directly suggested by the consideration that the regime we are interested in is one in which the nonlinear evolution of the wave competes with the defocusing effects associated with dispersion. The appropriate scaling is thus uniquely determined by imposing the constraint that the temporal evolution term, the nonlinear term, and the Hall term are at the same order in the magnetic induction equation. In addition, it is convenient to work in a moving frame, since this eliminates from the equations uninteresting translational motion terms. These conditions lead to the introduction of the following scaled variables:

$$X = \epsilon(x - Ct), \quad \tau = \tfrac{1}{2}\epsilon^2 t,$$

where C is the speed of the moving frame, and the factor $\frac{1}{2}$ in the definition of the slow variable τ is included in order to make a direct connection with the paper of Hada (1993).

The final important assumption concerns equipartition. The condition that β remain close to unity can be formally written as $c_s^2/c_A^2 - 1 = \epsilon\Delta$, where, as stated before, c_s is the average sound speed and Δ is a parameter of order unity.

Compatibility conditions determine the value of C: one finds $u_0 - C = \sigma = \pm 1$, where the plus (minus) sign stands for regressive (progressive) propagation with respect to the

orientation of the ambient magnetic field. We note that for the problem at hand $|u_0| \gg 1$, so that our reference frame practically moves with the bulk flow.

The computation is now straightforward: by equating terms at the first nontrivial order, we obtain

$$\frac{\partial u_1}{\partial \tau} = -\frac{\partial}{\partial X}\left(\Lambda u_1^2 - \sigma \Delta u_1 + |b_1|^2\right),$$

$$\frac{\partial b_1}{\partial \tau} = -\frac{\partial}{\partial X}(u_1 b_1) - \frac{i}{\xi}\frac{\partial^2 b_1}{\partial X^2}, \qquad (10)$$

together with $u_1 = -\sigma \rho_1$, $\rho_1 = p_1$, and $b_1 = \sigma v_1$. Here $\Lambda = (\lambda + 1)/2$ (see eq. [7]).

Equations (10) essentially coincide with those of Hada (1993), the only difference being the factor $1/\xi$ entering the dispersive term (and $u_0 \neq 0$). These equations describe the behavior of small-amplitude magnetic and velocity perturbations under the combined influence of nonlinearity and dispersion. Without the dispersive Hall term (and adding dissipation), they are reminiscent of the equations modeling MHD turbulence written by Thomas (1968).

3.2. Stability Diagram

Let us concentrate first on progressive propagation, which concerns waves excited by the disk rotation and propagating in the positive-x half-space.

It is immediately seen that the equations admit as solutions circularly polarized Alfvén waves, as in the linear case when the velocity (or equivalently the density) perturbations vanish at first order. In fact, $u_1 = 0$ and $b_1 = Ae^{i\phi}$, with $A = A_0 = $ constant, and $\phi = k_0 X - \omega_0 \tau$ satisfy the above equations, provided that $\omega_0 = -k_0^2/\xi$. Therefore, the same small-amplitude waves found in the linear case (the factor of 2 difference in the dispersion relation is related to the different definitions of the time variables) still persist after the introductions of the nonlinear terms. However, any small deviation from a perfectly constant amplitude for the magnetic perturbation induces a dynamical reaction in the system due to the coupling between velocity and magnetic perturbations.

It is thus important to analyze the stability properties of those waves under the influence of small changes in the amplitude A. The analysis is carried out writing $A = A_0 + \delta A$, $\phi = \phi_0 + \delta\phi$, $u_1 = 0 + \delta u$, and expanding to first order equations (10). The linear set of equations that obtains for the perturbations δA, $\delta\phi$, and δu (all of which are Fourier-decomposed as usual as $\sim e^{i(KX - \Omega\tau)}$) can be solved when the determinant $\mathscr{D}$ of the associated matrix vanishes. This leads as in Hada (1993) to a cubic equation. The long-wavelength limit $K \to 0$ of the equation $\mathscr{D} = 0$ can be shown to reduce to that of Hada with simply the wavenumber of the carrying wave k_0 changed into k_0/ξ in our case.

The main feature of Hada's (1993) linear stability diagram, namely, the antisymmetry of the unstable regions with respect to the origin in the $(k_0/\xi, \Delta)$-plane, is thus recovered as shown in Figure 1 From that figure, we see that the behavior of the system at fixed Δ under the effect of a small perturbation of the amplitude of the basic Alfvén waves changes from stability to instability when the sign of k_0 is changed, except for very small values of Δ, in which case the system is always stable.

The discussion can be repeated for the regressive propagation case in a completely analogous manner, retrieving exactly the same results, except for the fact that the stability
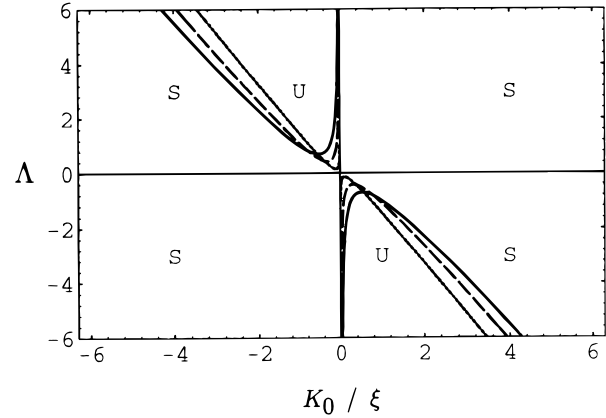

FIG. 1.—Linear stability diagram in the long perturbation wavelength limit for progressive wave propagation. The stability boundaries for three different normalized wave amplitudes A_0 are shown in the $(k_0/\xi, \Delta)$ parameter space. The solid line illustrates the case $A_0 = 1$, while the dotted and dash-dotted lines refer to the cases $A_0 = 0.2$ and $A_0 = 0.6$, respectively. The labels S and U in the figure stand for stable and unstable regions.

diagram in the $(k_0/\xi, \Delta)$-plane is reversed with respect to the k_0/ξ-axis.

The physical meaning of the above formal results and their implications for the phenomena under study are readily found, transforming back the magnetic variables to the original nonscaled reference frame fixed with respect to the star. The unperturbed circularly polarized wave in this frame can be written as

$$b_1(x, t) = b_x + ib_y = A_0 \exp\left\{ik_0\epsilon\left[x - \left(w_\pm + \epsilon\frac{\omega_0}{2k_0}\right)t\right]\right\},$$

where A_0 is real and $w_\pm = \pm|u_0| \pm 1$ is the dominant term of the phase velocity of the wave for the progressive and regressive waves, respectively. From the above expression it can be deduced that for both waves there is a one-to-one correspondence between the sign of the wavenumber k_0 and the polarization character of the carrying wave, being left-handed if $k_0 > 0$ and right-handed otherwise. Considering now one single propagation direction, the sign of k_0 changes with the sense of rotation impressed to the transverse component of the magnetic field. The dependence on the sign of k_0 of the onset of the modulational instability is therefore explained by considering the fact that the perturbed wave envelope will steepen only when the rotation of the transverse component agrees with the sense of the thermal ion motion around the basic magnetic field, since in that case a resonant amplification sets in.

In the physical system under study the sense of rotation impressed to the transverse component of the magnetic field is determined by the rotation of the disk, and it is therefore the same for both the waves propagating away from the central object. These waves, however, have opposite direction of propagation with respect to the ambient field and therefore opposite polarizations, and hence wavenumbers of opposite signs. Since, however, the stability diagram associated with opposite propagation is reversed with respect to k_0, it follows that, assuming the same plasma β on both sides, the waves traveling in the two opposite lobes show analogous stability/instability properties, developing instabilities or not depending on the relative angle between the angular momentum vector of the disk and the external uniform magnetic field. This picture is consistent with the

physical argument mentioned above: the instability arises when the rotation of the transverse component of the magnetic wavevector, which, as we have seen, is the same on both sides, agrees with the sense of thermal ion motion. The sense of rotation of ions, however, also does not change passing from one lobe to the other, due to the hourglass configuration of the zeroth-order field.

3.3. Numerical Exploration of the Nonlinear Regime

To see the further dynamical evolution of the system, we must go beyond the linear phase of the modulational instability. This allows us to confirm the basic asymmetry of the stability diagram and to investigate the behavior of the unstable waves for long timescales.

The numerical code utilized to integrate equations (10) was developed by one of us (F. B.) in order to investigate the nonlinear propagation of MHD waves in conditions in which the Hall term is relevant, together with a strong coupling between hydrodynamic and magnetic effects. The numerical code and some numerical tests are extensively described in Bacciotti, Passot, & Sulem (1996c), and only its main features are described here. The code is pseudo-spectral and is designed for the three-dimensional case, although in the present case it is used in its one-dimensional version. Several different schemes are implemented for the time stepping: after several tests, we chose as the most accurate for the case at hand a combination of exact temporal solutions for linear second-order terms and an Adams-Bashforth scheme for the nonlinear terms.

We followed the evolution of the various physical quantities through the nonlinear regime, starting always from the same initial conditions but varying the values of Δ and k_0/ξ, in order to verify whether the predictions of the linear stability analysis are still valid in the nonlinear regime, and what is the character of the instability.

We furthermore studied two different situations: the adiabatic case, for which we adopted a value of λ equal to the specific-heat ratio $\gamma = 5/3$ in equation (7), and a case that includes "radiative losses," as previously discussed, modeled as a first approximation by a polytropic law with a different value of the exponent, namely, $\lambda = \frac{1}{3}$. We concentrate here on progressive propagation.

The runs were made with a spatial grid of $N = 256$ regularly spaced points and temporal steps equal to 10^{-2} or 10^{-3}. The spatial scale was amplified and rescaled by a factor of 15 to reproduce correctly a long-wavelength perturbation on the amplitude of the carrying wave. The initial condition used was $u_i = 0.0$ for the velocity perturbation, while for the magnetic field we chose a circularly polarized wave modulated in amplitude by a Gaussian, in the form $b = b_y + ib_z = (1 + 0.05e^{-4(x-\pi)^2})e^{ik_0x}$. In the following it should be remembered that numerically $u_1 = \rho_1$, therefore the resulting density profiles are velocity profiles too. Since, as we will show, sharp fronts are readily formed, we add a viscous term of the form $v\partial^2 u_1/\partial x^2$ in the velocity equation in equations (10); at our resolution, a typical value used for v is 0.4. The ionization fraction for all these runs was kept constant at $\xi = 0.1$.

We explored various regions of the $(k_0/\xi - \Delta)$ parameter space, retrieving the same conditions for the growth of the instability predicted by the linear analysis. In Figures 2, 3, and 4 we illustrate the results for three representative cases, all with $\Delta = 4$. In Figure 2 we present the final spatial profile of the velocity at the time $\tau = 100$ for two unstable
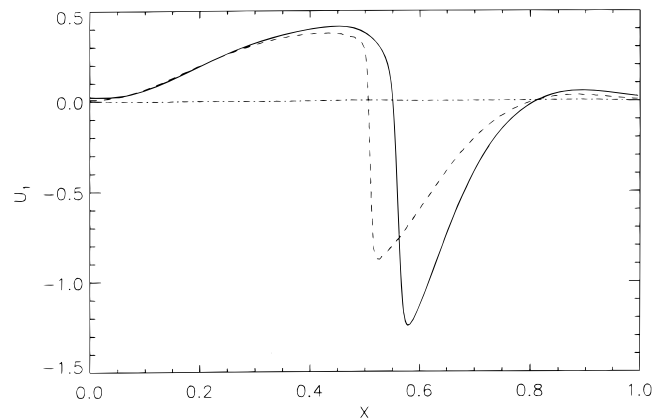

FIG. 2.—Spatial profile of the normalized velocity perturbation u_1 at the time $\tau = 100$ for the unstable cases $\Delta = 4$, $k_0/\xi = -2$, $\lambda = \frac{1}{3}$ (solid line) and $\Delta = 4$, $k_0/\xi = -2$, $\lambda = 5/3$ (dashed line), superimposed on the profile of the stable case $\Delta = 4$, $k_0/\xi = 2$ (dash-dotted line), which on this scale appears as a straight horizontal line.

cases with $k_0/\xi = -2$: the first one for the adiabitic case $\lambda = 5/3$ (dashed line) and the second one for $\lambda = \frac{1}{3}$ (solid line). The third (dot-dashed) line in the figure refers to the stable case $k_0/\xi = 2$. Figure 3 shows the velocity profile in the stable case on a stretched scale. Figure 4 illustrates the profiles of the magnetic perturbations (i.e., the wave envelope $b_y^2 + b_z^2$) for the same three cases.
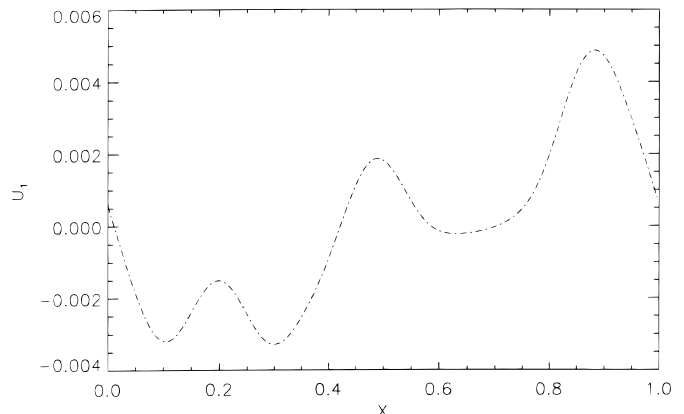

FIG. 3.—Spatial profile of the normalized velocity perturbation u_1 at the time $\tau = 100$ of the stable case $\Delta = 4$, $k_0/\xi = 2$, as in Fig. 2 but on a stretched velocity scale.
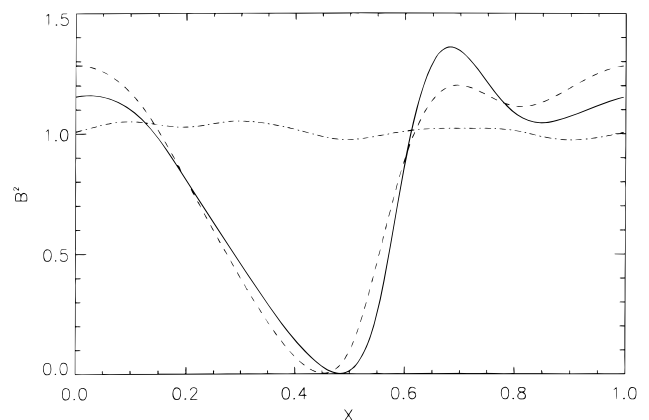

FIG. 4.—Spatial profile of the normalized wave envelope $B^2 = b_y^2 + b_z^2$ at the time $\tau = 100$ for cases identical to those in Fig. 2.

As can be readily seen, the development of the instability results in the formation of sharp fronts in the velocity/density profile of the first order (in ϵ) of the velocity/density perturbation. As expected, the radiative case develops stronger fronts. The perturbation of the magnetic amplitude is also subject to growth, both in the adiabatic and in the radiative cases. In the stable case, on the contrary, the perturbations never grow very far beyond the initial imposed value; this has been tested as well for times much longer than the ones displayed here.

3.4. Comparison with Observations

Even though in this paper we want to prove a point of principle rather than make a detailed comparison with the observations, we can use the results of the numerical simulations to check whether the instabilities that form are indeed capable of producing the conditions for the observed emission.

Absolute luminosity measurements of bright features of stellar jets are hardly found in the literature (the line intensity is intrinsically very weak, especially in the beam region we are modeling, and is very likely attenuated by an unknown amount of dust commonly present in star-forming regions). The most meaningful comparison with the observations that can be performed at this stage is therefore an estimate of the average relative luminosity contrast between the bright knot, which in the simulations is associated with the maximum of the density perturbation (ρ_M), and the weakly emitting region between a knot and the following one ("interknot" region), associated with the density minimum (ρ_m) in our plots.

We derived a representative value of the observed average luminosity contrast from the papers by Raga, Mundt, & Ray (1991) and Mundt, Ray, & Raga 1991, in which the authors present, for several well-known collimated jets, relative intensity tracings along the jet axis integrated across the jet in the light of the forbidden [S II] $\lambda\lambda 6716, 6731$ doublet. For each jet we determined the ratio $\Sigma = \bar{I}_m/\bar{I}_M$, where $\bar{I}_m$ and $\bar{I}_M$ are the average relative minima and maxima read on the tracings. Averaging then over all the jets, a mean ratio $\bar{\Sigma} \sim 0.4$ obtains.

This value has to be compared with the luminosity ratio given by our simulations. If the ionization fraction of the gas is assumed to be constant, the emissivity (ergs cm^{-3} s^{-1}) in a collisional forbidden line is roughly proportional to $\rho^2 T^{-1/2} \exp(-T_{exc}/T)$, where T is the gas temperature and $T_{exc} \sim 21{,}400$ K for the [S II] lines. In the adiabatic case both the variation of the density and that of the temperature contribute to the emissivity, while in the radiative case the excess heating radiated away on timescales much shorter than the dynamical timescales, and the compression at the shock front can be considered as isothermal (Draine & McKee 1993). Transforming back the numerical results into physical values, we estimated the ratio Σ between the calculated emissivity at the minimum and at the maximum as a function of ϵ, considering for the adiabatic case a reference temperature (intermediate between T_m and T_M) of 5000 K, and neglecting the temperature variation in the radiative case. The result is shown in Figure 5, where we plot both the adiabatic (*solid line*) and the radiative (*dashed line*) curves. It can be readily seen that the observed value $\bar{\Sigma} = 0.4$ can be obtained assuming $\epsilon \sim 0.15$ in the adiabatic case and $\epsilon \sim 0.23$ in the radiative one. These values of ϵ are consistent with the observed velocity fluctuation in the beams of
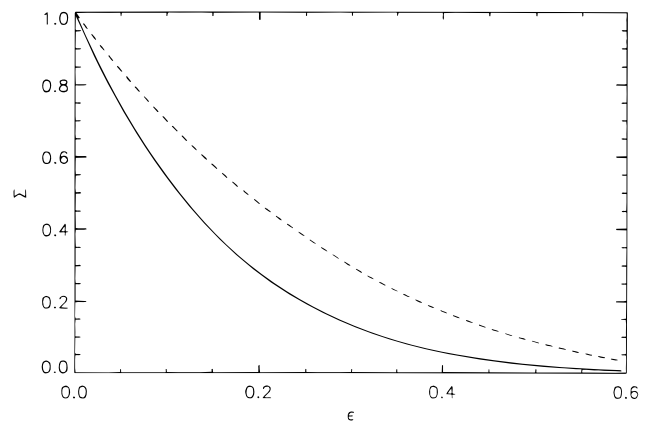

FIG. 5.—Ratio Σ between the emissivity at the density minimum and the emissivity at the density maximum as a function of ϵ, for the adiabatic case (*solid line*) and the radiative one (*dashed line*). The average value of Σ stemming from observations of jets is ~ 0.4.

various laboratory jets that are in the range 16%–30% (Arneodo et al. 1996). In addition, note that the obtained results actually refer to a limiting case, since we took $\Delta = 4$ and a very small initial amplitude perturbation in the envelope of the magnetic wave (5%). Results from other runs (not shown here) demonstrate that a smaller Δ (i.e., a case closer to equipartition) and/or a larger imposed initial perturbation would produce a stronger jump in ρ and this would produce the same observed luminosity contrast with a smaller ϵ.

The physical picture that emerges from the previous discussion is one in which circularly polarized Alfvén waves excited by the rotation of the accretion disk propagate away from the star in opposite directions with opposite polarities. If the plasma β is such that Δ has the same sign on both sides, these waves may develop into sharp compressions or weak shocks, which will generate heating and density enhancements on both lobes of the jet, while negligible effects develop in both lobes again for the other sign of Δ. This constitutes a simple, new-conception explanation for the optical and IR-emission of the nodular beam of protostellar jets, and for the fact that in some cases only the terminal bow shock is identified, while the linear section is not visible (Reipurth 1994; Bally, Morse, & Reipurth 1996).

4. DISCUSSION AND CONCLUSIONS

In this paper we propose a new possible physical mechanism to form flow perturbations in the beam section of a stellar jet, which could be described as mild compressions or very weak shocks, of the peculiar type required to justify the low-excitation emission of bright moving knots. The mechanism if based on the stability properties of Alfvén waves propagating in the partially ionized medium that fills the jet's channel.

Circularly polarized Alfvén waves are excited by the rotation of the circumstellar disk that twists the large-scale magnetic field perpendicular to the plane of the disk. The waves propagate inside the gas in opposite directions, and with opposite polarizations, since the sense of rotation impressed by the disk to the transverse components of the magnetic field is the same on both sides. We have shown that under the physical conditions present inside the jet the wave propagation is well described in the context of the MHD regime with the Hall term included in the magnetic induction equation, as a consequence of the partial ionization of

the medium. When quasi-equipartition between thermal and magnetic energies is assumed, the variables and the coordinates can be conveniently expanded to obtain a simplified, but still nonlinear, set of equations, suitable for the study of the evolution at large spatial and temporal scales of modulations of the initial wave amplitude. These modulations are plausibly occurring at the jet's base as a consequence of the sudden release of accumulated magnetic twist.

An analytical quasi-linear stability analysis shows that for quasi-parallel propagation modulational perturbations may develop instabilities for opposite signs of the wavenumber k_0 (uniquely correlated with the polarization of the carrying wave) and of the quantity Δ (see Fig. 1). However, if the sense of propagation is reversed, the stability diagram in the $(k_0/\xi, \Delta)$-space is also reversed with respect to the k_0/ξ-axis. Oppositely traveling waves have both opposite senses of propagation and opposite polarizations. If the plasma β has the same value on both sides of the star, and the large-scale magnetic field has the same direction and orientation (as is natural to assume following common cloud contraction models), the traveling waves will show the same stability/instability properties on both sides. In particular, they will develop or not develop instabilities, depending on the relative angle between the angular momentum vector of the disk and the external uniform magnetic field.

A numerical study of the equations in the full nonlinear regime reveals the character of the instability. Our simulations show that in the unstable parameter regime, sharp compression fronts do form in the flow, while in the stable case the perturbations remain bounded approximately to their initial value. Even in the limiting case of very small initial perturbations and without imposing strict equipartition, temperature/density perturbations associated with the instability do give rise to the average luminosity contrast observed in the jet beam between bright knots and interknot regions. In spite of the admitted crudeness of the assumptions made in this preliminary study, we believe that the idea of nonlinear steepening of modulational perturbations of Alfvén waves could constitute a promising alternative to the pure fluid mechanisms so far investigated to explain the peculiarities of the observed morphology of stellar jets. In addition, this model could provide an explanation for the puzzling observation that, in some cases, the linear jet sections are missing, even if the terminal bow shocks are present. This model could in principle help determine the actual direction of the magnetic field if future observations are able to resolve accretion disks and determine their sense of rotation. In fact, from the knowledge of the sense of rotation of the disk and the fact that the jet is observed together with the terminal bow shocks, one can deduce the actual direction of the magnetic field, in the framework of this model, at least when the plasma β can be assumed to be approximately the same on both sides.

A number of refinements and extensions of this work can be envisaged at the present stage. The inclusion of cylin-drical geometry together with the effects of weak dependence on transverse variables would be desirable, as well as that of a variable ionization fraction along the jet, as derived from the observations, for example in RW Aurigae (Bacciotti et al. 1996b) and in HH 34 (Bacciotti et al. 1996a). The observed variation (analyzed both empirically and with a phenomenological model), proportional to $1/(1 + x)$, where x is the distance from the star along the axis, could be introduced, although at some cost, since a new nonlinear term appears in the induction equation.

Finally, a puzzling and striking fact remains to be explained, namely, that the emission of stellar jets is often observed to be one-sided: it has been estimated that in about 50% of known cases a counterjet is barely seen, or not observable at all, in spite of the fact that matter is clearly ejected symmetrically, as evidenced by the presence of terminal bow shocks on both sides, located at approximately the same distance from the star and moving with comparable velocities in opposite directions (see, for example, the cases of HH 46/47 and HH 34 described in Reipurth & Heathcote 1991 and 1992, respectively). Extinction arguments, based on the projection of the jet axis with respect to the observer, combined with the location of the parent YSO at the rim of a dense cloud, do not always apply, since observations of monopolar jets at wavelengths influenced in a lesser way by dust extinction confirm the asymmetry of the phenomenon (Rodriguez & Reipurth 1994; Curiel et al. 1993). All this evidence points toward an intrinsic nature of the observed asymmetry, generated by a mechanism that, while leaving unaltered the basic properties of the ejection of matter, is capable of giving rise to different emissions in the two opposite lobes.

The physical theory in the form proposed here could justify an asymmetry only if the plasma β is significantly different on the opposite sides of the star or the magnetic field has a quadrupolar configuration at large scale. However, kinetic effects, such as nonlinear Landau damping, that have been investigated in the literature both in the high-β regime (Rogister 1971) and for the equipartition $\beta \sim 1$ case of interest here are known to introduce extra nonlinear and nonlocal terms in the DNLS equation (Mjølhus & Wyller 1986, 1988; Spangler 1989, 1990; Medvedev & Diamond 1996). The importance of the newly added terms depends on β, on the ratio of electronic to ionic temperatures, and on the degree of anisotropy of the pressure. Consideration of these effects could in principle lead to an asymmetry in the stability character of the traveling waves and, as a consequence, in the emission properties of the jet.

REFERENCES

Arnedo, A., et al. 1996, Europhys. Lett., 34, 411
Bacciotti, F., Chiuderi, C., & Oliva, E. 1995, A&A, 296, 185 (BCO)
Bacciotti, F., Eislöffel, J., & Ray, T. P. 1996a, in preparation
Bacciotti, F., Hirth, G. A., & Natta, A. 1996b, A&A, 310, 309
Bacciotti, F., Passot, T., & Sulem, P. L. 1996c, in preparation
Bally, J., Morse, J., & Reipurth, B. 1996, in Science with the Hubble Space Telescope. II, ed. P. Benvenuti, F. D. Macchetto, & E. J. Schreier (Baltimore: STScI)
Braginskii, S. 1965, in Reviews of Plasma Physics, Vol. 1 ed. M. Leontovich (New York: Consultants Bureau), 205
Curiel, S., Rodríguez, L. F., Moran, J. M., & Cantò, J. 1993, ApJ, 415, 191
Dalgarno, A., & McCray, R. A. 1972, ARA&A, 10, 375
Draine, B. T., & McKee, C. F. 1993, ARA&A, 31, 373
Draine, B. T., Roberge, W. G., & Dalgarno, A. 1983, ApJ, 264, 485
Elmegreen, B. G. 1991, ApJ, 378, 139
Hada, T. 1993, Geophys. Res. Lett., 20, 2415

Hartigan, P., Morse, J., & Raymond, J. 1994, ApJ, 436, 125
Kaup, D. J., & Newell, A. C. 1978, J. Math. Phys., 19, 798
Königl, A. 1995, in Lecture Notes in Physics 465, Disk and Outflows around Young Stars, ed. S. Beckwith, J. Staude, A. Quetz, & A. Natta (Berlin and Heidelberg: Springer), 282
Lovelace, R. V. E., Berk, H. L., & Contopoulos, J. 1991, ApJ, 379, 696
Lovelace, R. V. E., Wang, J. C. L., & Sulkanen, M. E. 1987, ApJ, 315, 504
Medvedev, M. V., & Diamond, P. H. 1996, Phys. Plasmas, 3, 863
Mjølhus, E. 1978, J. Plasma Phys., 19, 437
Mjølhus, E., & Wyller, J. 1986, Phys. Scripta, 33, 442
———. 1988, J. Plasma Phys., 40, 229
Mundt, R. 1993, in Proc. Sixth Int. Workshop of the OAC on Stellar Jets and Bipolar Outflows, ed. L. Errico & A. Vittone (Dordrecht: Kluwer), 91
Mundt, R., Ray, T. P., & Raga, A. C. 1991, A&A, 252, 740
Passot, T., Vazquez, E., & Pouquet, A. 1995, ApJ, 455, 536
———. 1996, ApJ, in press
Pelletier, G., & Pudritz, R. E. 1992, ApJ, 394, 117
Pudritz, R. E., & Norman, C. 1986, ApJ, 301, 571
Raga, A. C. 1991a, in The Physics of Star Formation and Early Stellar Evolution, ed. C. J. Lada & N. D. Kylafis (Dordrecht: Kluwer), 247
———. 1991b, AJ, 101, 1472

Raga, A. C., Mundt, R., & Ray, T. P. 1991, A&A, 252, 733
Ray, T. P. 1987, A&A, 171, 145
Reipurth, B. 1989, in ESO Workshop on Low Mass Star Formation and Pre–Main Sequence Objects, ed. B. Reipurth (Garching: ESO), 247
———. 1994, A General Catalogue of Herbig-Haro Objects, electronically published via anon.ftp to ftp.hq.eso.org, directory/pub/Catalogs/Herbig-Haro
Reipurth, B., & Heathcote, S. R. 1991, A&A, 246, 511
———. 1992, A&A, 257, 693
———. 1993, in Astrophysical Jets, ed. D. Burgarella, M. Livio, & C. O'Dea (Cambridge: Cambridge Univ. Press)
Rodríguez, L. F., & Reipurth, B. 1994, A&A, 281, 882
Rogister, A. 1971, Phys. Fluids, 14, 2733
Spangler, S. 1985, ApJ, 299, 122
———. 1989, Phys. Fluids B, 1, 1738
———. 1990, Phys. Fluids B, 2, 407
Spangler, S., & Sheerin, J. 1982, J. Plasma Phys., 27, 193
Strom, K. M., Strom, S. E., Wolff, S. C., Morgan, J., & Wenz, M. 1986, ApJS, 62, 39
Thomas, J. 1968, Phys. Fluids, 11, 1245
Vazquez, E., Passot, T., & Pouquet, A. 1995, ApJ, 441, 702
Uchida, Y., & Shibata, K. 1985, PASJ, 37, 515